A Journal of the Gesellschaft Deutscher Chemiker

Angewandte International Edition Chemie

GDCh

www.angewandte.org

Accepted Article

Title: Product Selectivity Controlled by Steric Adsorption in Zeolite Micropores over a Pd@Zeolite Catalyzed Hydrogenation of Nitroarene

Authors: Jian Zhang, Liang Wang, Yi Shao, Yanqin Wang, Bruce Gates, and Feng-shou Xiao

To be cited as: *Angew. Chem. Int. Ed.* 10.1002/anie.201703938
Angew. Chem. 10.1002/ange.201703938

Link to VoR: http://dx.doi.org/10.1002/anie.201703938
http://dx.doi.org/10.1002/ange.201703938

WILEY-VCH

10.1002/anie.201703938

WILEY-VCH

Product Selectivity Controlled by Steric Adsorption in Zeolite Micropores over a Pd@Zeolite Catalyzed Hydrogenation of Nitroarene

Jian Zhang, Liang Wang,* Yi Shao, Yanqin Wang, Bruce C. Gates, and Feng-Shou Xiao*

Abstract: This work delineates the persuasive example for controlling the steric adsorption of molecules on metal nanoparticles by zeolite crystals, thus enhancing the product selectivity in hydrogenation of reactants with more than one reducible group. Key to this success is by fixing Pd nanoparticle inside of Beta zeolite crystals to form a fixed structure (Pd@Beta). In the hydrogenation of substituted nitroarenes with multiple reducible groups as model reaction, the Pd@Beta exhibits superior selectivity for the hydrogenation of the nitro group, outperforming both conventional Pd nanoparticles supported on zeolite crystals and a commercial Pd/C catalyst. The extraordinary selectivity of Pd@Beta is reasonably attributed to the steric adsorption of nitroarenes on Pd nanoparticle controlled by zeolite micropores, as elucidated by competitive adsorption and adsorbate-displacement FT-IR tests. Importantly, the strategy is general and extensible to synthesize selective Pt and Ru catalysts by fixing inside of Beta and mordenite zeolites.

For most of a century, metal-catalyzed hydrogenation reactions have attracted the attention of researchers because of their importance in industrial production of chemicals and fuels.[1-4] Numerous supported transition metals catalyze the hydrogenation of compounds such as olefins, aromatic hydrocarbons, carboxylic acids, aldehydes, and ketones,[4-8] but when more than one reducible group is present in the reactant (such as in a nitroaromatic compound), most hydrogenation catalysts are non-selective. To overcome this limitation, inorganic additives (e.g., Pb and V) have been incorporated in the heterogeneous catalysts,[9] blocking undesirable side reactions by partially covering the active surface sites, but at the expense of reducing the hydrogenation activity.[9b] Recently, organic additives such as soluble compounds with N- or S-containing groups have been introduced into these metal catalysts,[10] changing the mode of adsorption of the reactant molecules on the metal sites in ways that improve the selectivities. However, it is a challenge to tune the adsorption mode and to minimize the leaching of the organic groups from the metal surface.

Zeolite, which has been widely applied in the petrochemical industry, is famous for the shape-selective catalysis,[3b,11] where the molecules are sterically adsorbed and selectively transformed in the uniform zeolite micropores, thus giving unusual product selectivities in various reactions. However, rare efficient strategies exist so far, which allows for employing zeolite to rationally control the steric adsorption of reactants on metal nanoparticle catalysts.

In this work, we report a methodology for selective hydrogenation by sterically controlling the adsorption on metal@zeolite core-shell catalysts, whereby the advantages of metal nanoparticles with high catalytic activities and zeolite micropores facilitating selective adsorption of reactants are synergistically combined. By employing hydrogenation of substituted nitroarenes as model reactions, an industrially important class of reaction for producing valuable functionalized anilines,[4,6a,7,12-14] Pd nanoparticles fixed inside the regular porous structure of crystalline zeolite Beta (Pd@Beta) give both high activities and excellent selectivities combined with long catalyst lifetimes. In contrast, conventional supported Pd catalysts are non-selective and lack stability. The extraordinary selectivities observed for Pd@Beta are attributed to the unique sterically guided adsorption of nitroarenes in the zeolite Beta micropores.

Scheme S1 shows procedures for synthesis of Pd@Beta by a seed-directed route, whereby zeolite Beta crystal-supported Pd nanoparticles function as zeolite seeds in a gel that has the composition 11 Na_2O/Al_2O_3/26 SiO_2/270 H_2O. Because the seed-directed synthesis of zeolite Beta crystals proceeds by a core-shell growth mechanism,[15] the newly formed zeolite grows from the seeds of Beta crystals containing Pd nanoparticles, giving fixing the Pd nanoparticles inside of the zeolite crystals (Pd@Beta). In this case, the Pd nanoparticles are larger than the zeolite Beta micropore diameters, which is beneficial for fixing the Pd nanoparticles within the zeolite framework.[16] In contrast, the classic encapsulation of metals in zeolites involves the formation of metal clusters within the zeolite micropores.[17,18]

Figure 1A shows a scanning electron microscopy (SEM) image of Pd@Beta, demonstrating the uniform morphology. XRD pattern and N_2 sorption isotherms (Figures S1 and S2, Table S1) confirm the high purity of the highly crystalline Pd@Beta. The scanning transmission electron microscopy (STEM) image gives direct evidence of the Pd nanoparticles within Pd@Beta (Figure 1B). Energy dispersive spectroscopy (EDS) analysis of the Pd@Beta crystallization process confirms the core-shell growth directed by the Pd-containing seed to form the fixed structure (Scheme S2, Figure S3). The data show clearly that the synthesis technique completely prevents the formation of metal nanoparticles on the external surfaces of the catalyst particles—they are all encapsulated and subject to the steric control of the zeolite pores that provide the only access to the metal surface. Tomographic images of Pd@Beta (Figures 1C-E) confirms the encapsulation; the Pd nanoparticles can be observed directly, fully encapsulated inside of the zeolite Beta crystals. The images further show that the Pd nanoparticles with significantly brighter contrast than the zeolite crystals, are highly dispersed inside of the zeolite crystals, with a distribution of

[a] J. Zhang, Dr. L. Wang, Prof. F.-S. Xiao
Department of Chemistry
Zhejiang University
Hangzhou 310028, Zhejiang, China
E-mail: liangwang@zju.edu.cn; fsxiao@zju.edu.cn
[b] Y. Shao, Prof. Y. Wang
Shanghai Key Laboratory of Functional Materials Chemistry,
Research Institute of Industrial Catalysis, School of Chemistry and Molecular Engineering
East China University of Science and Technology
Shanghai 200237, China
[c] B. C. Gates
Department of Chemical Engineering
University of California, Davis
CA 95616, USA

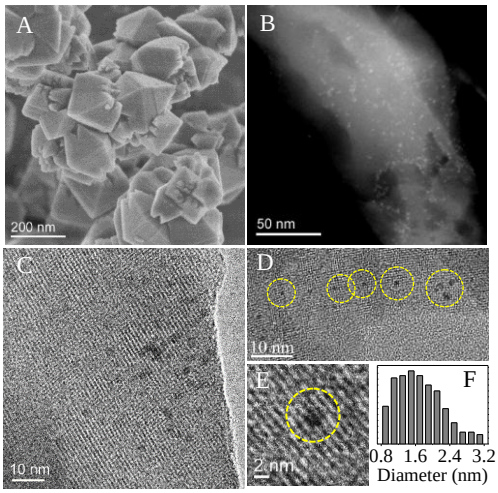

Figure 1. (A) SEM, (B) STEM, (C-E) HR-TEM images of Pd@Beta. The yellow cycles highlighted the Pd nanoparticle. (F) The size distribution of Pd nanoparticles on Pd@Beta.

diameters of 0.9-3.1 nm (Figures 1F and S4), which is very similar to the sizes of Pd nanoparticles on the seed (Pd/seed Beta, Figure S5), suggesting the Pd nanoparticles are stable during the zeolite crystallization. In the tomographic image of the conventionally prepared Pd/zeolite Beta, the Pd nanoparticles exist only on the external surface of the zeolite crystals (Figure S6). Complementary data show that Pd@Beta has excellent thermal stability. Even when calcined in air for 4 h at 600 °C, the Pd nanoparticle size distribution of the sample remains similar to that of the as-synthesized Pd@Beta (Figures S7A and B). All these results demonstrate that the Pd nanoparticles are stably fixed inside of the zeolite crystals (Figure S8). In contrast, the conventionally prepared Pd nanoparticles on the external surface of zeolite Beta crystals become much larger (2-13 nm) after the same treatment (Figures S7C and D).

The zeolite pore diameters are small enough (~6.7 Å) that at the zeolite-metal interface they can constrain molecules interacting with the metal. Thus, the performance of the catalyst is expected to depend on how the reactants adsorb on the metal. Figure 2A shows catalytic conversion of 4-nitrochlorobenzene to 4-chloroaniline in the presence of various Pd-containing catalysts, whereby the selective hydrogenation of the nitro group (to give 4-chloroaniline) is a highly desirable practical goal. Normally, dechlorination occurs on the conventional supported Pd catalysts (Pd/C, Pd/TiO_2, Pd/Al_2O_3, and Pd/SiO_2, Figures S9 and S10), giving aniline as a by-product. As a result, the conventional catalysts exhibit 4-chloroaniline selectivities ranging from 70.9% to 89.6%. Significantly, Pd@Beta displays selectivity greater than 99.0%, and 4-chloroaniline is the sole product. These results suggest that Pd@Beta favors the reduction of nitro groups over chloro groups in our reactants (Table S2). Similar results were also observed in the hydrogenation of nitroarenes incorporating carbonyl groups, with 4-nitrobenzaldehyde used as a model reactant (Figure 2B). Again, Pd@Beta exhibits excellent selectivity, with that to 4-aminobenzaldehyde being greater than 99.0%. If the Pd nanoparticles are not encapsulated with the zeolite crystals, the Pd/zeolite Beta gives very low selectivity for the aniline (1.6%).

To understand origin of the high selectivity over Pd@Beta catalyst, the Pd nanoparticle sizes of Pd@Beta and Pd/Beta are artificially adjusted (Figures S11 and S12), while a series of Pd@Beta catalysts with different Pd particle sizes always exhibited superior selectivity than Pd/Beta catalysts in the hydrogenation of 4-nitrochlorobenzene and 4-nitrobenzaldehyde (Table S3), demonstrating the insensitivity of Pd nanoparticle size for the high selectivity of Pd@Beta. It is reasonably suggested that the high selectivity of Pd@Beta should be directly attributed to the Pd nanoparticles encapsulated with zeolite structure rather than other factors. To confirm this suggestion, partial destruction of the Beta zeolite framework on Pd@Beta by HF was carried out (Figure S13), the treated Pd@Beta-HF exhibits obviously reduced 4-aminobenzaldehyde selectivity (41.5%, Table S4), compared with the as-synthesized Pd@Beta (>99.5%), demonstrating the importance of zeolite sheath for enhancing the selectivity.

Furthermore, IR spectra of various compounds adsorbed on the catalysts were investigated, as shown in Figure S14. When solely nitrobenzene or chlorobenzene was used as adsorbate, Pd/C and Pd@Beta gave spectra with obvious peaks at 1525-1529 and 1346-1362 cm^{-1}, assigned to the N=O bond of nitrobenzene or at 741 cm^{-1}, assigned to the C-Cl bond of chlorobenzene.[5b,14a] These results show that both catalysts adsorb each of the compounds. In competitive adsorption of mixtures of chlorobenzene and nitrobenzene (Figure S15A), the IR spectrum of the Pd/C exhibits the bands of both nitro (1525 and 1346 cm^{-1}) and chloro group (741 cm^{-1}), indicating simultaneous adsorption of chlorobenzene and nitrobenzene. But, significantly, the IR spectrum of the Pd@Beta gives evidence of bands of only the nitro group (1529 and 1362 cm^{-1}), indicating the selective adsorption of nitrobenzene on Pd@Beta. Similar results were observed in competitive adsorption tests carried out with mixed benzaldehyde and nitrobenzene,

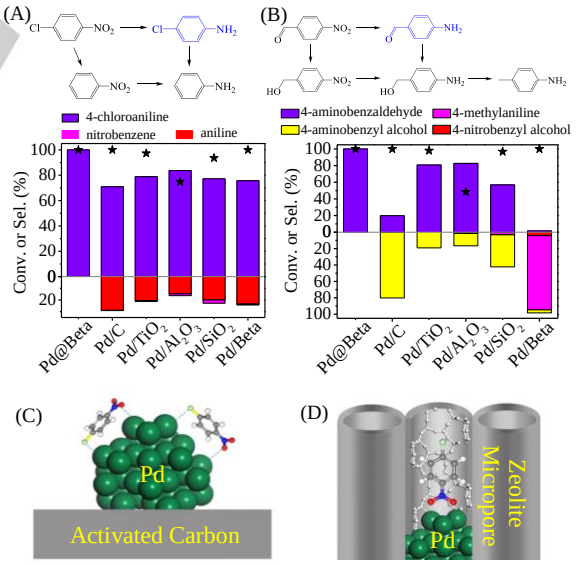

Figure 2. Data of substrate conversion (the black stars) and product selectivities (the colorized columns) characterizing the hydrogenation of (A) 4-nitrochlorobenzene and (B) 4-nitrobenzaldehyde with various catalysts. Reaction conditions: 1 mmol of substrate, 0.2 mol% Pd catalyst, 10 mL of toluene, 1 MPa H_2, 110 ℃ for 45 min in hydrogenation of 4-nitrochlorobenzene, 80 °C for 2 h in the hydrogenation of 4-nitrobenzaldehyde. Proposed model of 4-nitrochlorobenzene adsorbed on (C) Pd/C and (D) Pd@Beta. The blue, red, light green, dark green, gray, white circles represent N, O, Cl, Pd, C, and H atoms, respectively.

whereby the Pd@Beta selectively adsorbs nitrobenzene whereas Pd/C adsorbs both (Figure S15B). These results demonstrate a unique feature of the Pd@Beta for selective adsorption of nitrobenzene and account for the catalyst's superior selectivity in the hydrogenation of nitroarenes.

We did further experiments to elucidate the role of the zeolite fixing the Pd nanoparticles by doing adsorbate-displacement tests. The results determine the adsorption selectivity and adsorption strengths of nitrobenzene and chlorobenzene on encapsulated and conventional Pd catalysts. Typically, in these experiments, a solid Pd catalyst was mounted in a cell with Ar flowing through it. After adsorption of one reactant in the presence of flowing Ar for a fixed interval, a second reactant was introduced into the Ar stream, giving it the opportunity to displace the first as an adsorbate. As shown in Figure S16A, the chlorobenzene initially adsorbed on Pd@Beta is readily displaced by nitrobenzene. The IR spectrum of the Pd@Beta with chlorobenzene initially includes a band at 741 cm^{-1} assigned to the C-Cl bond, indicating its strong adsorption. But when nitrobenzene was introduced, the 741 cm^{-1} band quickly disappeared, being replaced by bands characteristic of nitro groups (1529 and 1360 cm^{-1}), indicating the efficient displacement of the adsorbed chlorobenzene by nitrobenzene. On the other hand, in the attempted reverse experiment, with nitrobenzene adsorbed first on the Pd@Beta, chlorobenzene did not displace it (Figure S16B)—the IR bands of adsorbed nitrobenzene (1522 and 1360 cm^{-1}) always remained stronger than those of any adsorbed chlorobenzene (741 cm^{-1}), even after long times of flow of chlorobenzene and even at a high temperature of 300 °C, indicating that chlorobenzene was highly inefficient in displacing the nitrobenzene on Pd@Beta and that nitrobenzene was much more strongly adsorbed on Pd@Beta than chlorobenzene. In contrast, when the catalyst was Pd/C, with its readily accessible Pd surface, the displacement of chlorobenzene by nitrobenzene and the reverse both occurred rapidly (Figures S17A and B), demonstrating the lack of adsorption selectivity for these compounds on the conventional catalyst Pd/C. These results are bolstered by results of competitive adsorption tests (Figure S15) and *operando* Raman spectra (Figures S18 and S19).

In view of these results, and because pure Beta zeolite without Pd nanoparticles evidences no specific and strong adsorption of the reactants, as shown by adsorption-replacement IR spectra measured with zeolite Beta (Figure S20), we conclude that the zeolite sheath influences the accessible Pd surface and the bonding of reactants to it. It is well known that nitroarene molecules commonly adsorb with the aromatic ring parallel to the metal surface.[5b] When 4-nitrochlorobenzene was adsorbed on Pd/C, both chloro- and nitro-groups might interacted with the Pd sites. The parallel adsorption of 4-nitrochlorobenzene on the surface of Pd nanoparticles, with both the nitro- and chloro- groups interacting with Pd sites (Figure 2C), could give hydrogenation of both groups. In contrast, when 4-nitrochlorobenzene is adsorbed on Pd@Beta, we infer that the molecule is parallel to the microporous channels due to the structure confinement (Scheme S3, Figure 2D). Thus, the zeolite micropores change the sterics of the molecular adsorption on Pd sites in contact with these micropores, leading to the bonding of 4-nitrochlorobenzene to the Pd sites *via* the nitro group rather than chloro group because of the stronger interaction of the nitro group than of chloro group with the metal surface, as confirmed by the Raman spectra (Figure S19).

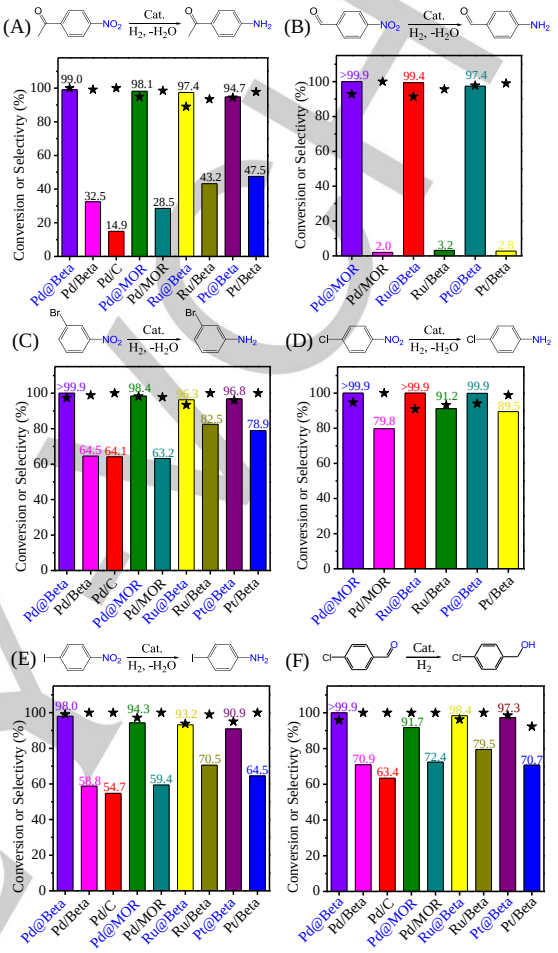

Figure 3. Data of substrate conversion (the black stars) and product selectivities (the colorized columns with numeral values) characterizing the hydrogenation of variously substituted nitroarenes and chlorobenzaldehyde with different catalysts.

Pd leaching is a general problem for many supported catalysts, and their stabilities and recyclabilities are critical for industrial applications. Interestingly, the Pd@Beta shows stable catalytic performances in the recyclable tests and undetectable Pd leaching or aggregation in long-term flow tests (See Figures S21-23 and Table S5 for details), outperforming the commercial Pd/C catalyst. Figure 3 shows the catalytic performances in hydrogenation of variously substituted nitroarenes and chlorobenzaldehydes (Figures 3A, C, E, and F, see Tables S6 and S7 for detailed data and reaction conditions) as well as benzophenone (Figure S24) over various catalysts. Typically, the Pd@Beta catalyst is generally active and selective. For example, in the hydrogenation of 4-acetonitrobenzene, Pd@Beta displays selectivity to 4-aminoacetophenone at 99.0% with full conversion of 4-acetonitrobenzene, while the Pd/Beta and Pd/C exhibits much lower selectivities to 4-aminoacetophenone at 32.5 and 14.9%, respectively (Figure 3A). Similar phenomena were also observed in the hydrogenation of 3-bromonitrobenzene and 4-iodonitrobenzene, where Pd@Beta exhibits higher selectivity to the corresponding substituted

aniline products than Pd/C and Pd/Beta (Figures 3C and E). Even in the hydrogenation of nitroarenes with *ortho*-substituted groups, such as 2-chloronitrobenzene, the Pd@Beta still displays the selectivity to 2-aminochlorobenzene at over 99.5%, much higher than that of 74.2% over the Pd/Beta (Table S8). These data demonstrate the universality of the Pd@Beta for the selective hydrogenation of various nitroarenes with substituted groups at different positions (*meta, ortho,* and *para*), due to the specific adsorption of nitro group of these molecules on the Pd sites in the Pd@Beta (Table S8, Figure S25).

Recent works summarize typical metal-containing (e.g. Au, Co, Pt, Fe and bimetallic hybrids) heterogeneous catalysts for selective hydrogenation of nitroarenes with hydrogen,[5,6,7a] but it is rarely achieved on heterogeneous monometallic Pd catalysts with both high activity and excellent selectivity.[19] Here, fixing metal nanoparticles inside of zeolite crystals open the way to obtain a series of heterogeneous catalysts with high activity and selectivity simultaneously, such as Pd@MOR (MOR is zeolite mordenite), Ru@Beta, and Pt@Beta (Figure S26), all with uniformly distributed metal nanoparticles, as confirmed by TEM tomography images (Figures S27-S29). Significantly, the Pd@MOR, Ru@Beta, and Pt@Beta catalysts all display outstanding selectivities in the hydrogenation of various substituted nitroarenes and chlorobenzaldehyde (Figure 3, see Table S7 for detailed data and reaction conditions), and these values are much greater than those of Pd/MOR, Ru/Beta, and Pt/Beta obtained by impregnation methods (Figure S30). These results taken together demonstrate the generality of the synthesis and catalytic efficacy of metals@zeolites.

In summary, we report a novel strategy to improve the selectivity of Pd nanoparticles in the hydrogenation of substituted nitroarenes by using a core-shell Pd@Beta catalyst obtained from a Pd-containing seed-directed synthesis of zeolite crystals. Because the zeolite micropores control the steric adsorption of substrate molecules on the Pd sites, the Pd@Beta exhibits outstanding selectivity and extraordinary stability for the hydrogenation of substituted nitroarenes to the corresponding anilines. The metals@zeolites catalysts reported here appear to open the way to developing a class of highly selective metal catalysts.

Acknowledgements

This work is supported by National Natural Science Foundation of China (91634201, 21403192 and 91645105).

Keywords: zeolite • heterogeneous catalyst • Pd nanoparticle • selective hydrogenation

[1] a) L. Shao, W. Zhang, M. Armbruester, D. Teschner, F. Girgsdies, B. Zhang, O. Timpe, M. Friedrich, R. Schlögl, D. S. Su, *Angew. Chem., Int. Ed.* **2011**, *50*, 10231-10235; b) H. Guan, J. Lin, B. Qiao, X. Yang, L. Li, S. Miao, J. Liu, A. Wang, X. Wang, T. Zhang, *Angew. Chem., Int. Ed.* **2016**, *55*, 2820-2824; c) M. De bruyn, S. Coman, R. Bota, V. I. Parvulescu, D. E. De Vos, P. A. Jacobs, *Angew. Chem., Int. Ed.* **2003**, *42*, 5333-5336.

[2] a) M. Behrens, F. Studt, I. Kasatkin, S. Kühl, M. Hävecker, F. Abild-Pedersen, S. Zander, F. Girgsdies, P. Kurr, B.-L. Kniep, M. Tovar, R. W. Fischer, J. K. Nørskov, R. Schlögl, *Science* **2012**, *336*, 893-897; b) Q. Yang, Q. Xu, S. Yu, H.-L. Jiang, *Angew. Chem., Int. Ed.* **2016**, *55*, 3685-3689.

[3] a) A. D. Schmitz, G. Bowers, C. S. Song, *Catal. Today* **1996**, *31,* 45-46; b) C. S. Song, *Catal. Today* **2003**, *86,* 211-263; c) X. Wang, M. Li, C. Cao, C. Liu, J. Liu, Y. Zhu, S. Zhang, W. Song, *ChemCatChem* **2016**, *8*, 3224-3228.

[4] A. Corma, S. Iborra, A. Velty, *Chem. Rev.* **2007**, *107*, 2411-2502.

[5] a) A. Corma, P. Serna, *Science* **2006**, *313*, 332-334; b) M. Boronat, P. Concepción, A. Corma, S. González, F. IIlas, P. Serna, *J. Am. Chem. Soc.* **2007**, *129*, 16230-16237; c) A. Corma, P. Serna, P. Concepción, J J. Calvino, *J. Am. Chem. Soc.* **2008**, *130*, 8748-8753.

[6] a) R. V. Jagadeesh, A.-E. Surkus, H. Junge, M.-M. Pohl, J. Radnik, J. Rabeah, H. Huan, V. Schünemann, A. Brückner, M. Beller, *Science* **2013**, *342***,** 1073-1076; b) F. A. Westerhaus, R. V. Jagadeesh, G. Wienhöfer, M. M. Pohl, J. Radnik, A.-E. Surkus, J. Rabeah, K. Junge, H Junge, M. Nielsen, A. Brückner, M. Beller, *Nat. Chem.* **2013**, *5*, 537-543

[7] a) H. Wei, X. Liu, A. Wang, L. Zhang, B. Qiao, X. Yang, Y. Huang, S. Miao, J. Liu, T. Zhang, *Nat. Commun.* **2015**, *5*, 5634; b) J. Gu, Z. Zhang P. Hu, L. Ding, N. Xue, L. Peng, X. Guo, M. Lin, W. Ding, *ACS Catal.* **2015**, *5*, 6893-6901; c) X. Liu, H. Li, S. Ye, Y. Liu, H. He, Y. Cao, *Angew. Chem., Int. Ed.* **2014**, *53*, 7624-7628.

[8] M. Zhao, K. Yuan, Y. Wang, G. Li, J. Guo, L. Gu, W. Hu, H. Zhao, Z. Tang, *Nature* **2016**, *539*, 76-80.

[9] a) H. Zhang, X.-K. Gu, C. Canlas, A. J. Kropf, P. Aich, J. P. Greeley, J. W. Elam, R. J. Meyers, J. A. Dumesic, P. C. Stair, C. L. Marshall, *Angew. Chem., Int. Ed.* **2014**, *53*, 12132-12136; b) U. Siegrist, P. Baumeister, H. U. Blaser, M. Studer, *Chemical Industries*, (Ed.: F. Herkes), Marcel Dekker, New York, **1998**, pp. 207-220.

[10] a) S. T. Marshall, M. O'Brien, B. Oetter, A. Corpuz, R. M. Richards, D. K. Schwartz, J. W. Medlin, *Nat. Mater.* **2010**, *9*, 853-858; b) B. Wu, H. Huang, J. Yang, N. Zheng, G. Fu, *Angew. Chem., Int. Ed.* **2012**, *51*, 3440-3443.

[11] a) K. Lee, S. H. Cha, S. B. Hong, *ACS Catal.* **2016**, *6*, 3870-3874; b) Y. Roman-Leshkov, M. Moliner, J. A. Labinger, M. E. Davis, *Angew. Chem., Int. Ed.* **2010**, *49*, 8954-8957.

[12] a) D. Cantillo, M. Baghbanzadeh, C. O. Kappe, *Angew. Chem., Int. Ed.* **2012**, *51*, 10190-10193; b) H. Zhu, X. Ke, X. Yang, S. Sarina, H. W. Liu *Angew. Chem., Int. Ed.* **2010**, *49*, 9657-9661.

[13] a) K. Shimizu, Y. Miyamoto, A. Satsuma, *J. Catal.* **2010**, *270*, 86-94; b) M. J. Beier, J.-M. Andanson, A. Baiker, *ACS Catal.* **2012**, *2,* 2587-2595.

[14] a) L. Wang, J. Zhang, H. Wang, Y. Shao, X. Liu, Y. Wang, J. P. Lewis, F.-S. Xiao, *ACS Catal.* **2016**, *6*, 4110-4116; b) A. Mori, T. Mizusaki, M. Kawase, T. Maegawa, Y. Monguchi, S. Takao, Y. Takagi, H. Sajiki, *Adv Syn. Catal.* **2008**, *350*, 406-410.

[15] B. Xie, H. Zhang, C. Yang, S. Liu, L. Ren, L. Zhang, X. Meng, B. Yilmaz, U. Muller, F.-S. Xiao, *Chem. Commun.* **2011**, *13*, 3945-3947.

[16] A. B. Laursen, K. T. Højholt, L. F. Lundegaard, S. B. Simonsen, S. Helveg, F. Schüth, M. Paul, J.-D. Grunwaldt, S. Kegnæs, C. H. Christensen, K. Egeblad, *Angew. Chem., Int. Ed.* **2010**, *49*, 3504-3507.

[17] a) S. Goel, S. I. Zones, E. Iglesia, *J. Am. Chem. Soc.* **2014**, *136*, 15280-15290; b) S. Goel, Z. Wu, S. I. Zones, E. Iglesia, *J. Am. Chem. Soc.* **2012**, *134*, 17688-17695; c) N. Wang, Q. Sun, R. Bai, X. Li, G. Guo, J. Yu, *J. Am. Chem. Soc.* **2016**, *138*, 7484-7487.

[18] L. Liu, U. Díaz, R. Arenal, G. Agostini, P. Concepción, A. Corma, *Nat. Mater.* **2016**, *16*, 132-138.

[19] S. Zhang, C.-R. Chang, Z.-Q. Huang, J. Li, Z. Wu, Y. Ma, Z. Zhang, Y. Wang, Y. Qu, *J. Am. Chem. Soc.* **2016**, *138*, 2629-2637.

10.1002/anie.201703938

WILEY-VCH

Entry for the Table of Contents

COMMUNICATION

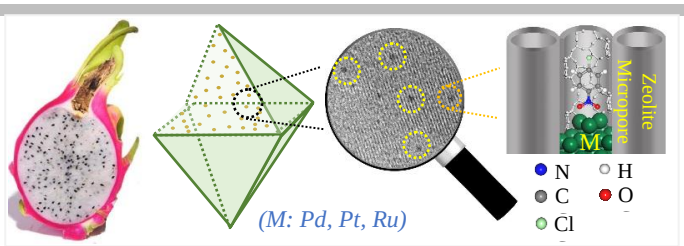

Pitaya-like structure enhances the selectivity: Pd nanoparticle fixed inside of Beta zeolite crystals (Pd@Beta) exhibits superior selectivity in the hydrogenation of substituted nitroarenes with multiple reducible groups, which is reasonably attributed to the steric adsorption of nitroarenes on Pd nanoparticle controlled by zeolite micropores.

Jian Zhang, Liang Wang, Yi Shao, Yanqin Wang, Bruce C. Gates, and Feng-Shou Xiao**

Page No. – Page No.
Product Selectivity Controlled by Steric Adsorption in Zeolite Micropores over a Pd@Zeolite Catalyzed Hydrogenation of Nitroarene